

# CRYSTAL AND MOLECULAR STRUCTURE STUDIES ON SOME ORGANIC COMPOUNDS OF MEDICAL INTEREST

**Synopsis submitted to the Madurai Kamaraj University  
for the award of the degree of**

**DOCTOR OF PHILOSOPHY  
IN  
PHYSICS**

By

**M. VENKATESHAN**

(Regn. No: P4124)

(Ref.No: R2/PT/Reg/Physics/15)

*Under the Guidance of*

**Dr. J. Suresh M.Sc., M.Phil., P.B.D.C.A., B.Ed., Ph.D.,  
Principal & Associate Professor of Physics  
The Madura College, Madurai - 11.**



**Madurai Kamaraj University**  
*(University with Potential for Excellence)*  
**Madurai - 625021, Tamilnadu, India.**

October 2020

---

This thesis titled “*Crystal and Molecular structure studies on some organic compounds of medical interest*” is based on the research work carried out by the author at the Department of Physics, The Madura College (Autonomous), Madurai - 625 011 under the supervision of **Dr. J. Suresh**, Principal & Associate Professor of Physics, The Madura College during the period 2015-2020.

In the present work, crystal structures of Sixteen organic compounds were elucidated and investigated. For the elucidation of the crystal structures, single crystal X-ray diffraction technique is used. Seven groups of compounds were organized suitably in various chapters as given below. Part 2 deals with the homology modeling of RNA dependent RNA polymerase (RdRp) from SARS (Severe Acute Respiratory Syndrome) CoV-2 (Corona Virus – 2) and docking studies with the small molecule inhibitors: pyridine, azafluorene, azaphenanthrene, pyrrolidine, triazole and cinnamoyl derivatives. For the elucidation of the structures of these molecules at atomic resolution, single crystal X-ray diffraction techniques were employed.

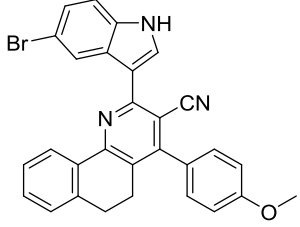
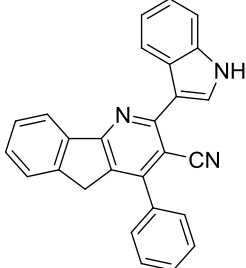
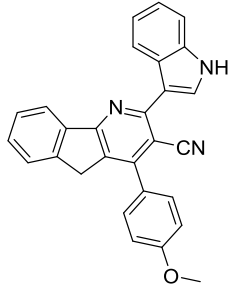
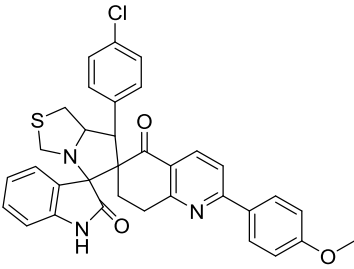
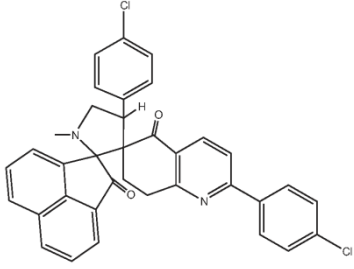
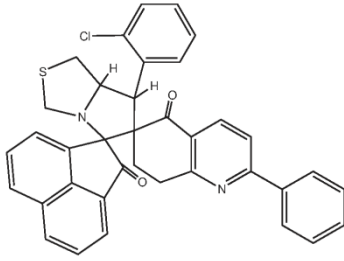
**Chapter 1** deals with the general introduction about X-ray crystallography, instrumentation, data collection techniques, data reduction and correction procedures, structure solution methods and refinement procedures. Also, the list of crystallographic programmes used and the general procedure followed to solve the structures presented in this thesis are explained.

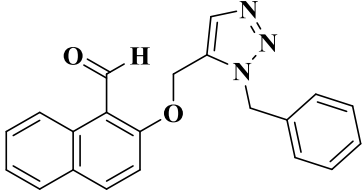
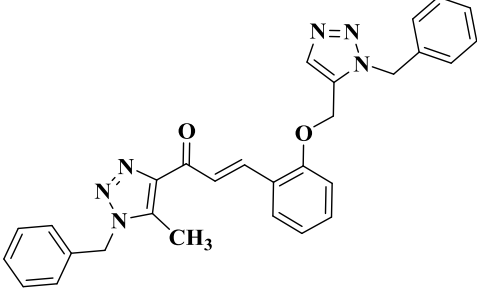
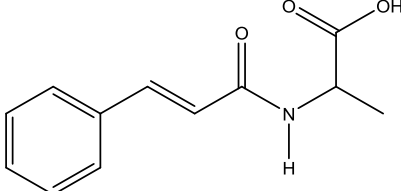
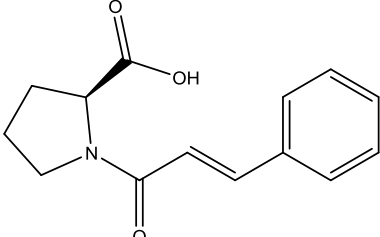
In (**Chapters 2 to 8**) of this thesis, the X-ray crystal structures of a few indole substituted pyridine-3-carbonitrile, azafluorene, azaphenanthrene, pyrrolidine, triazole and cinnamoyl derivatives are reported. Their intermolecular interactions were analyzed using Hirshfeld surface analysis, QTAIM (Quantum Topological Atoms In Molecules) and NCI (Non-Covalent Interaction) index. Frontier molecular orbitals were analyzed using DFT

(Density Functional Theory). The crystal data along with the R-factors of the crystal structures of the compounds are given in Table 1.

The crystal structures reported are:

series	Structure	Name
1		2-(5-bromo-1H-indol-3-yl)-4-(4-fluorophenyl)-5,6,7,8,9,10-hexahydrocycloocta[b]pyridine-3-carbonitrile
2		4-(4-fluorophenyl)-2-(1H-indol-3-yl)-5,6,7,8,9,10-hexahydrocycloocta[b]pyridine-3-carbonitrile
3		2-(1H-indol-3-yl)-4-(thiophen-2-yl)-5,6,7,8,9,10-hexahydrocycloocta[b]pyridine-3-carbonitrile
4		4-(2,6-difluorophenyl)-2-(1H-indol-3-yl)-1,4,5,6,7,8,9,10,11,12,13,14-dodecahydrocycloclododeca[b]pyridine-3-carbonitrile
5		2-(5-bromo-1H-indol-3-yl)-4-(4-chlorophenyl)-5,6,7,8,9,10,11,12,13,14-decahydrocycloclododeca[b]pyridine-3-carbonitrile
6		2-(1H-indol-3-yl)-4-phenyl-5,6-dihydrobenzo[h]quinoline-3-carbonitrile

7		2-(5-bromo-1H-indol-3-yl)-4-(4-methoxyphenyl)-5,6-dihydrobenzo[h]quinoline-3-carbonitrile
8		2-(1H-indol-3-yl)-4-phenyl-5H-indeno[1,2-b]pyridine-3-carbonitrile
9		2-(1H-indol-3-yl)-4-(4-methoxyphenyl)-5H-indeno[1,2-b]pyridine-3-carbonitrile
10		7'-(4-chlorophenyl)-2''-(4-methoxyphenyl)-7',7a',7'',8''-tetrahydro-1'H,3'H,5''H-dispiro[indoline-3,5'-pyrrolo[1,2-c]thiazole-6',6''-quinoline]-2,5''-dione
11		2'', 4'-Bis(4-chlorophenyl)-1'-methyl-7'',8''-dihydro-2H,5''H-dispiro[acenaphthylene-1,2'-pyrrolidine-3',6''-quinoline]-2,5''-dione
12		7'-(2-chlorophenyl)-2''-phenyl-7',7a',7'',8''-tetrahydro-1'H,2H,3'H,5''H-dispiro[acenaphthylene-1,5'-pyrrolo[1,2-c]thiazole-6',6''-quinoline]-2,5''-dione

13		2-((1-benzyl-1H-1,2,3-triazol-5-yl)methoxy)-1-naphthaldehyde
14		(E)-3-(2-((1-benzyl-1H-1,2,3-triazol-5-yl)methoxy)phenyl)-1-(1-benzyl-5-methyl-1H-1,2,3-triazol-4-yl)prop-2-en-1-one
15		cinnamoylalanine
16		cinnamoyl-L-proline

**Chapter 2** (Indole substituted hexahydrocycloocta[b]pyridine-3-carbonitrile derivatives) Pyridines assume much importance in organic synthesis because of the occurrence of their saturated and partially saturated derivatives in biologically active compounds and natural products such as nucleotides, pyridoxol (vitamin B6), and pyridine alkaloids. Substituted pyridines have also found a number of applications such as anticorrosion agents, insecticides and as potential drug substances. The *in-vitro* studies of pyridine carbonitrile exhibits anti-cancer properties against a series of cell lines. Also, cyanopyridine is a major scaffold for designing various chemotherapeutic agents. This

---

chapter describes the structural details of compounds 1 to 3. The compounds 1 & 2 crystallized in monoclinic system with  $P2_1/n$  spacegroup. The compound 3 belongs to trigonal with R-3H. In all the three structures, the cyclooctane ring adopts a twist-boat-chair. The pyridine ring in all the compounds is effectively planar. In the case of compounds 2 and 3, during the refinement of the structure, electron density peaks were located, close to inversion centers that were believed to be highly disordered solvent molecules, possibly ethyl acetate. Attempts to model the solvent molecules were not successful. The residual electron density was difficult to model and therefore, the SQUEEZE function of PLATON was used to eliminate the contribution of the electron density in the solvent region from the intensity data and the solvent-free model was employed for the final refinement. The crystal structures are stabilized through the intermolecular C-H...N and N-H...N interactions. The energy values of these interactions were predicted using QTAIM. Compound 1 forms a stronger interaction than the other two compounds. Also, the drug-like nature of compound 1 is higher than other compounds of this group, which is confirmed by molecular orbital analysis.

**Chapter 3** (Decahydrocyclododeca[b]pyridine-3-carbonitrile derivatives) The pyridine skeleton attracts more importance among chemists and biologists because of its abundance in nature. The naturally occurring pyridine containing compounds have various applications in pharmaceuticals. The organic compounds containing pyridine are an important class of HIV drugs, which inhibit RNA dependent DNA polymerase, and hence act as reverse transcriptase inhibitors. Some ruthenium complexes of pyridine show anti-cancer, anti-tumor and anti-viral activities. 1,4-Dihydropyridine derivatives have yielded many drugs which act as calcium channel agonists or antagonists and various bioactive compounds such as vasodilator, anti-atherosclerotic, antitumor, geroprotective, heptaprotective and anti-diabetic

---

agents. This chapter describes the structural details of compounds 4 and 5. The compound 4 crystallized in the monoclinic crystal system with  $P2_1/n$  space group while the compound 5 crystallized in the triclinic system with  $P-1$  space group. Initial structural solution showed co-crystallized solvent molecule for which a suitable model could not be found for the compound 5. Therefore, the data set was treated with SQUEEZE (Spek, 2015) routine of PLATON (Spek, 2009) to model the electron density in the void region. In compound 4, the 1,4-dihydropyridine adopts a shallow boat conformation and the pyridine ring (N1/C1-C5) in compound 5 is effectively planar. In compound 4, the cyclododecane ring adopts  $[1_{\text{enc}}2333]$  conformation; while in compound 5 it adopts distorted  $[1_{\text{enc}}3323]$  conformation. The compound 4 is stabilized through two  $N-H \dots N$  interactions. In compound 5 the molecules appear to be linked together through the  $C-H \dots Cl$  and  $C-H \dots \pi$  interactions.

**Chapter 4** (Azafluorene derivatives) Azafluorenes have attracted researchers towards its side by showing some moderate to good biological activities. The alkaloid extracted from the plant *Polyalthia debilis* contains 4-azafluorene derivatives showed anti-microbial, anti-malarial and cytotoxic activities. Naturally obtained *onychine* showed anti-fungal activity against *candida albicans* also anti-microbial activity against *Staphylococcus aureus*. This chapter describes the structural details of compounds 6 and 7. Both the compounds crystallized in the triclinic crystal system with  $P-1$  space group. Initial structural solution showed co-crystallized completely disordered solvent molecule (DMSO) which was modeled and refined using PART command along with a free variable. The solvent molecule is disordered over two sets of sites in a 0.515(2):0.485(3) ratio. In both the compounds, the azafluorene ring is essentially planar. The molecular structure of compound 6 is stabilized

---

through an intermolecular interaction N – H ... N. In compound 7, the host and guest molecules are forming two intermolecular interactions viz., N – H ... O and C – H ... O.

**Chapter 5** (Azaphenanthrene derivatives) Azaphenanthrene is a heterocyclic compound containing quinoline moiety. There are many quinoline derived drug candidates are best selling drugs in the market. They are advised for treating various medical conditions. The most promising property of quinoline derivatives is anti-malarial property. Bisquinoline, ferrochloroquine and chloroquinolinythiourea are found to possess good anti-malarial property. The *in-vitro* and *in-vivo* studies showed some dihydroquinoline with the inhibition property against farnesyltransferase which can control the cell proliferation in breast cancer cell assay. This chapter describes the structural details of compounds 8 and 9. Both the compounds crystallized in the triclinic crystal system with P-1 space group. Initial structural solution showed co-crystallized completely disordered solvent molecule (DMSO) which was modeled and refined using PART command along with a free variable. The solvent molecule is disordered over two sets of sites in a 0.792(2):0.208(2) ratio. In both the structures, the azaphenanthrene ring adopts planar conformation. The molecular structure of compound 8 is stabilized through an intermolecular interaction N – H ... N. In compound 9, the host and guest molecules are forming two intermolecular interactions viz., N – H...O and C – H...O.

**Chapter 6** (Pyrrolidine derivatives) Spiro-compounds represent an important class of naturally occurring substances, which in many cases exhibit important biological properties. Pyrrolidine derivatives are widely used as organic catalysts and also serve as important structural units in biologically active molecules. Acenaphthene derived compounds attracts the interest by having some important biological activities like anti-inflammatory, anti-tumor, anti-microbial and anti-fungal. This chapter describes the structural details of compounds 10



---

to 12. Compound 10 crystallized in the triclinic crystal system with P-1 space group and other two compounds were crystallized in the monoclinic system with  $P2_1/C$  (compound 11) and  $C_c$  (compound 12) space group. Initial structural solution showed co-crystallized solvent molecule for which a suitable model could not be found in the compounds 10 and 11. Therefore, the data set was treated with SQUEEZE (Spek, 2015) routine of PLATON (Spek, 2009) to model the electron density in the void region. The asymmetry unit of compound 10 contains two crystallographically independent molecules (molecules A and B). The pyrrolidine ring of molecule A adopts twisted conformation and molecule B adopts envelope conformation. In compounds 11 and 12, this ring adopts envelope conformation. The compound 10 is stabilized through N—H...N hydrogen bond and a series of C—H...O hydrogen bonds. In compound 11, the crystal is stabilized through one through one intermolecular C – H...O. There is no strong intermolecular interactions are observed in compound 12. Thus, this compound is stabilized through weak short contacts.

**Chapter 7** (1-benzyl-4-methyl-1H-1,2,3-triazole derivatives) Triazoles are an important class of heterocycles, commonly available in two isomeric forms viz., 1,2,3-triazole and 1,2,4-triazole, which drawn attention due to their broad spectrum of pharmacological activities. Gil and co-workers synthesized some 1,2,3-triazole derivatives, which showed better anti-tubercular activity against H37Rv strain than commercial *Rifampin*. Triazole derivatives showed anti-microbial, anti-fungal, analgesic, anti-inflammatory, anti-convulsant, anti-viral, anti-malarial, anti-cancer and anti-HIV properties. This chapter describes the structural details of compounds 13 and 14. Both the compounds are crystallized in the monoclinic crystal system with  $P2_1/n$  (Compound 13) and  $P2_1/c$  (compound 14) space group. In both the compounds, all the five- and six-membered rings are effectively planar. In

---

compound 13, the oxygen O2 acts as a double acceptor thus forming two C – H ... O intermolecular interactions. The compound 14 has C – H ... N and C – H ... O intermolecular interactions that stabilize the crystal.

**Chapter 8** (Cinnamoyl derivatives) In naturally occurring phenolic acids the predominantly known types are the derivatives of benzoic and cinnamic acids. Because of their abundance and low toxicity index cinnamoyl derivatives have been screened for their pharmacological activities had showed some good pharmacological activities. In general the phenol containing compounds have antioxidant properties because of their high redox potential. The antioxidant properties of derivatives of hydroxycinnamic acids are higher than its counterpart of benzoic acid. This chapter describes the structural details of compounds 15 and 16. The compound 15 crystallized in the monoclinic crystal system with  $P2_1/c$  space group while the compound 16 crystallized in the trigonal system with the  $P3_1$  space group. For compound 16, in the final refinement cycles, the structure was refined as an inversion twin using TWIN/BASF commands with the BASF value of -0.13501. This delivered the final, absolute structure parameter called Flack parameter 'x' of -0.1(15). The pyrrolidine ring in compound 16 adopts  $C_s$ -C12 <sup>$\beta$</sup> -exo conformation. The compound 15 is stabilized through two O – H ... O and two N – H ... O interactions. The compound 16 is stabilized through three O – H ... O and three C – H ... O interactions.

The intermolecular interaction strengths are qualified and quantified using Hirshfeld surface analysis, QTAIM and NCI analysis. The drug-likeness of the compounds are predicted on the basis of frontier molecular orbital analysis. The results of these analyses are discussed in all the chapters (Chapters 2 to 8).

### **Part 2:** Homology modeling and Molecular docking analysis

This part describes the process of homology modeling of SARS CoV-2 RdRp using SARS CoV RdRp (PDB id: 6NUR\_A) as a template for modeling. The modeled structure was energy minimized and validated before docking. Also, the docking of pyridine-3-carbonitrile, azafluorene, azaphenanthrene, pyrrolidine, triazole and cinnamoyl derivatives along with some approved drugs having anti-viral property and some phytochemicals are discussed.

## Synopsis

**Table 1 Crystal data of the organic compounds reported in Part I (Chapters 2 to 8)**

No.	Compound No.	a (Å)	b (Å)	c (Å)	$\alpha$ (°)	$\beta$ (°)	$\gamma$ (°)	Sp. Group	R-Index
1.	<i>Compd. 1</i>	10.8550(11)	10.9522(10)	18.533(2)	90	93.141(3)	90	P2 <sub>1</sub> /n	0.0424
2.	<i>Compd. 2</i>	9.8089(9)	11.7127(10)	18.9564(17)	90	99.813	90	P2 <sub>1</sub> /n	0.1048
3.	<i>Compd. 3</i>	30.3228(14)	30.3228(14)	12.1946(6)	90	90	120	R-3:H	0.0832
4.	<i>Compd. 4</i>	11.5752(7)	7.8182(4)	28.9629(17)	90	101.362(2)	90	P2 <sub>1</sub> /n	0.0735
5.	<i>Compd. 5</i>	10.3508(7)	12.2904(8)	12.6339(8)	81.09(2)	87.801(2)	78.354(2)	P $\bar{1}$	0.0675
6.	<i>Compd. 6</i>	9.5662(5)	10.4295(5)	11.4163(6)	90.3(3)	105.005(3)	115.95(3)	P $\bar{1}$	0.051
7.	<i>Compd. 7</i>	9.9760(6)	11.0573(5)	12.9317(7)	76.737(3)	68.739(3)	78.469(3)	P $\bar{1}$	0.499
8.	<i>Compd. 8</i>	9.3339(7)	10.4957(8)	12.2704(8)	82.964(3)	71.834(3)	64.713(3)	P $\bar{1}$	0.0538
9.	<i>Compd. 9</i>	10.5600(3)	11.2058(3)	12.7280(3)	83.158(2)	78.515(2)	69.156(2)	P $\bar{1}$	0.0383
10.	<i>Compd. 10</i>	11.8222(7)	14.7535(9)	19.5055(12)	68.396(3)	78.555(3)	87.302(3)	P $\bar{1}$	0.0579
11.	<i>Compd. 11</i>	8.8375(3)	28.3154(10)	13.3441(4)	90	94.552(3)	90	P2 <sub>1</sub> /c	0.056
12.	<i>Compd. 12</i>	18.7091(10)	17.8970(9)	9.2619(4)	90	107.146(2)	90	Cc	0.0388
13.	<i>Compd. 13</i>	14.013(3)	5.4123(11)	22.901(5)	90	93.157(5)	90	P2 <sub>1</sub> /n	0.0462
14.	<i>Compd. 14</i>	15.1962(17)	10.3077(11)	17.258(2)	90	108.616(3)	90	P2 <sub>1</sub> /c	0.0463
15.	<i>Compd. 15</i>	7.6748(13)	14.278(3)	20.476(4)	90	94.795(6)	90	P2 <sub>1</sub> /c	0.0451
16.	<i>Compd. 16</i>	15.9976(10)	15.9976(10)	13.4251(7)	90	90	120	P 31	0.0464

## Synopsis

---

Based on the above inferences, the following articles have been published in peer-reviewed international journals:

1. Azaphenanthrene derivatives as inhibitor of SARS CoV-2 Mpro: Synthesis, physicochemical, quantum chemical and molecular docking analysis  
**M. Venkateshan**, J. Suresh, M. Muthu & R. Ranjith Kumar  
(2020). *Chem. Data. Collec.* 28, 100470. (<https://doi.org/10.1016/j.cdc.2020.100470>)
2. Azafluorene derivatives as inhibitors of SARS CoV-2 RdRp: Synthesis, physicochemical, quantum chemical, modeling and molecular docking analysis  
**M. Venkateshan**, M. Muthu, J. Suresh & R. Ranjith Kumar  
(2020). *J. Mol. Struct.* 1220, 128741. (<https://doi.org/10.1016/j.molstruc.2020.128741>)
3. 2-[(1-Benzyl-1H-1,2,3-triazol-4-yl)methoxy]-1-naphthaldehyde  
R. Vishnupriya, **M. Venkateshan**, J. Suresh, G. Jaabil, A. Ponnuswamy & P. L. Nilantha Lakshman  
(2019). *IUCrData*. 4, x191525. (<https://doi.org/10.1107/S2414314619015256>)
4. Crystal structure, Hirshfeld surface analysis, DFT calculations and molecular docking studies on pyridine derivatives as potential inhibitors of NAMPT.  
**M. Venkateshan**, R. Vishnu Priya, M. Muthu, J. Suresh & R. Ranjith Kumar  
(2019). *Chem. Data. Collec.* 23, 100262. (<https://doi.org/10.1016/j.cdc.2019.100262>)
5. Synthesis, physicochemical and quantum chemical studies on a new organic NLO crystal: Cinnamoylproline  
**M. Venkateshan** & J. Suresh.  
(2019). *J. Mol. Struct.* 1180, 826-838.  
(<https://doi.org/10.1016/j.molstruc.2018.12.071>)
6. Crystal structure of 7'-(4-chlorophenyl)-2''-(4-methoxyphenyl) -7',7a',7'',8''-tetrahydro-1'H,3'H,5''H-dispiro[indoline-3,5'-pyrrolo[1,2-c]-thiazole-6',6''-quinoline]-2,5''-dione and an unknown solvent.  
R. Vishnupriya, **M. Venkateshan**, J. Suresh, R. V. Sumesh, R. Ranjith Kumar & P. L. Nilantha Lakshman.  
(2019). *Acta Cryst. E.* 75, 189-193. (<https://doi.org/10.1107/S2056989019000112>)